Long-Range Heavy-Ion Potential Induced by Multiple Coulomb Excitation

P. Fröbrich and R. Lipperheide
Hahn-Meitner-Institut für Kernforschung, Berlin West, Germany, and Freie Universität Berlin, Berlin West, Germany

and

H. Fiedeldey
Department of Physics, University of South Africa, Pretoria, South Africa
(Received 9 April 1979)

A Coulomb polarization potential is obtained by solving the inverse problem for the elastic component of the Coulomb-excitation S matrix. It takes account of multiple excitation and, for heavier systems, exhibits significantly less absorption than existing single-excitation potentials.

The large Coulomb fields present in heavy-ion collisions generally cause Coulomb excitation of one or both collision partners. In the elastic channel this leads to specific polarization and absorption effects[1-3] which can be described in terms of a long-range dynamic "Coulomb polarization potential." Such (complex) potentials have first been introduced phenomenologically.[1] A derivation of Coulomb polarization potentials from the theory of Coulomb excitation, assuming single-excitation processes only, has been given by Love, Terasawa, and Satchler[4] and Baltz *et al.*[5] These potentials describe adequately, e.g., the elastic scattering cross section for the system $^{18}O + ^{184}W$ at $E = 90$ MeV,[2] where indeed only the Coulomb transition to the lowest 2^+ state of ^{184}W affects the elastic scattering. For heavier systems, however, multiple Coulomb-excitation processes are important.[6] When these are taken into account, a derivation of the polarization potential along the lines of Refs. 4 and 5 becomes practically impossible.

In this Letter, we present a local, complex, l-independent potential which fully describes the effects of multiple Coulomb excitation. This potential is determined by a new method which consists in solving the inverse problem for the elastic component of the multiple Coulomb-excitation S matrix, for which calculational schemes are readily available.[7] When applied to the "single-excitation system" $^{18}O + ^{184}W$, the procedure essentially verifies the results of Ref. 4 (referred to as LTS in the following), and, via the determination of the l-independent equivalent of the l-dependent potential of Ref. 5, affords a direct comparison between the potentials of Refs. 4 and 5. More importantly, in "multiple-excitation systems" such as $^{40}Ar + ^{238}U$ at $E = 240$ MeV, it yields a polarization potential which deviates quite significantly from the LTS form.

We employ the inversion method proposed by Lipperheide and Fiedeldey.[8] The following parametrization of the (nonunitary) elastic scattering function at fixed energy as a function of angular momentum $l = \lambda - \frac{1}{2}$ is used:

$$S_l = S(\lambda) = \prod_{n=1}^{N} \left(\frac{\lambda^2 - \beta_n^2}{\lambda^2 - \alpha_n^2} \right), \tag{1}$$

where α_n, β_n are complex with $\mathrm{Re}\{\alpha_n, \beta_n\} \geq 0$. The function S represents the elastic component of the Coulomb-excitation S matrix divided by the Rutherford scattering function. It turns out, for the cases considered here, that the parametrization (1) represents the scattering function S_l (for l real) obtained from the Coulomb-excitation calculation[7] to very high accuracy.

The local, l-independent, complex potential uniquely associated with the S function (1) is determined iteratively by (cf. Sect. 2.4 of Ref. 8)

$$V(r) = \sum_{n=1}^{N} V^{(n)}(r), \tag{2}$$

$$V^{(n)}(r) = i\left(\frac{2E_{\mathrm{c.m.}}}{k^3 r}\right) \frac{d}{dr}\left[\frac{1}{r} \frac{\beta_n^2 - \alpha_n^2}{\bar{L}_n(r) + L_n(r)}\right], \quad n = 1, \ldots, N, \tag{3}$$

where the functions $L_n(r)$, $\bar{L}_n(r)$ are found by solving

$$\begin{aligned} -(i/k) dL_n/dr - L_n^2 + 1 - V^{(n-1)}/E_{\mathrm{c.m.}} - (\alpha_n^2 - \tfrac{1}{4})/(kr)^2 = 0, \\ (i/k) d\bar{L}_n/dr - \bar{L}_n^2 + 1 - V^{(n-1)}/E_{\mathrm{c.m.}} - (\beta_n^2 - \tfrac{1}{4})/(kr)^2 = 0, \end{aligned} \tag{4}$$

with $L_n, \bar{L}_n \to 1$ for $r \to \infty$. The starting potential $V^{(0)}(r)$ is the Rutherford potential. The complex poles α_n (zeros β_n) which happen to lie in the "anomalous" fourth (first) quadrant are not treated by the quantal inversion method of Eqs. (1)–(4) directly, but are first transformed to the first (fourth) quadrant by writing $(\lambda^2 - \alpha_n^2) = S_{\alpha_n}^{-1}(\lambda)(\lambda^2 - \alpha_n^{*2})$, where $S_{\alpha_n}(\lambda) = (\lambda^2 - \alpha_n^{*2})/(\lambda^2 - \alpha_n^2)$ is a unitary S function associated classically with a real potential[9] (analogously for β_n).

We remark that in the cases considered here, we were also able to reproduce our results to good accuracy with the help of a purely classical inversion procedure for complex potentials.[10]

(i) $^{18}O + ^{184}W$ *at* $E = 90$ *MeV.*[2]—Figure 1(a) shows the elastic component S_l of the Coulomb excitation S matrix calculated with the help of the de Boer–Winther code,[7] using a rotor model with $B(E2) = 37\,600$ MeV fm^2. It is found that S_l is affected appreciably only by the 2^+ state. The Rutherford scattering function has been divided out. This S function is generally reproduced by the LTS potential except for small l, where LTS obtain too much absorption (cf. Fig. 9 of Ref. 4).

A practically perfect fit to the function $S_l = S(\lambda)$ was obtained using expression (1) with $N = 3$. The potential calculated according to Eqs. (2)–(4) is shown in Fig. 1(b). Its imaginary part practically coincides with the (purely imaginary) LTS potential.

The elastic cross section calculated from the polarization potential $V(r)$ (added to the Rutherford potential) is shown in Fig. 1(c). The corresponding LTS cross section (Fig. 8 of Ref. 4) essentially agrees with ours.

For the present case of single Coulomb excitation it is of interest to consider also the l-dependent polarization potential of Ref. 5. In order to compare it directly with the l-independent potentials $V^{\mathrm{LTS}}(r)$ and $V(r)$, we calculated from it the scattering function and determined the corresponding l-independent potential $V^{\mathrm{BKGP}}(r)$ (Ref. 5) with the help of our inversion method. The imaginary parts of V^{LTS} and V^{BKGP} are shown in Fig. 2. The imaginary part of our potential, ImV, coincides with V^{BKGP} over the entire relevant region, 11 fm $\lesssim r \lesssim$ 30 fm; it differs from V^{LTS} near the nuclear surface and for larger r. This proves that the BKGP potential is essentially "exact" in the single-excitation limit.

(ii) $^{40}Ar + ^{238}U$ *at* $E = 240$ *MeV.*—In this system, multiple-Coulomb-excitation effects are predominant. It appears that so far no detailed knowledge of the corresponding polarization potential

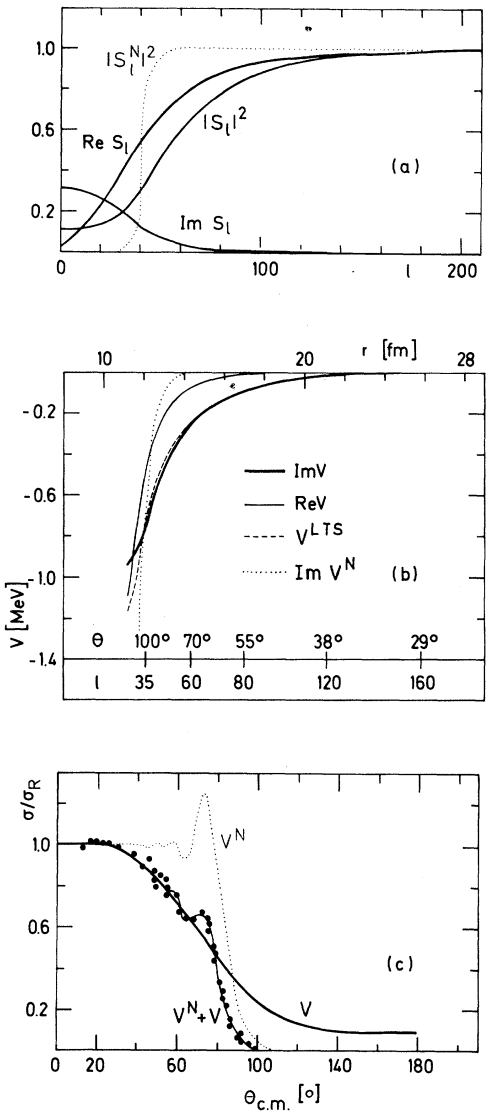

FIG. 1. The system $^{18}O + ^{184}W$ at $E = 90$ MeV. (a) Scattering function: The solid curves show the real and imaginary parts of the elastic component S_l of the Coulomb-excitation S matrix as well as the corresponding reflection function $|S_l|^2$; the dotted curve represents the nuclear reflection function $|S_l^N|^2$ computed from a nuclear potential V^N with parameters given in Fig. 8 of Ref. 2. (b) Potential: The solid curves show the real and imaginary parts of the potential V calculated by inversion of S_l; for comparison, the dashed curve shows the LTS potential V^{LTS}, and the dotted curve, the imaginary part of V^N; the θ, l scale corresponds to Rutherford orbits. (c) Cross section: The heavy solid curve shows the elastic cross section corresponding to V alone; the dotted curve represents the cross section computed from V^N alone, while the thin solid line shows the elastic cross section corresponding to $V + V^N$; the dots represent the experimental data (Refs. 1 and 2).

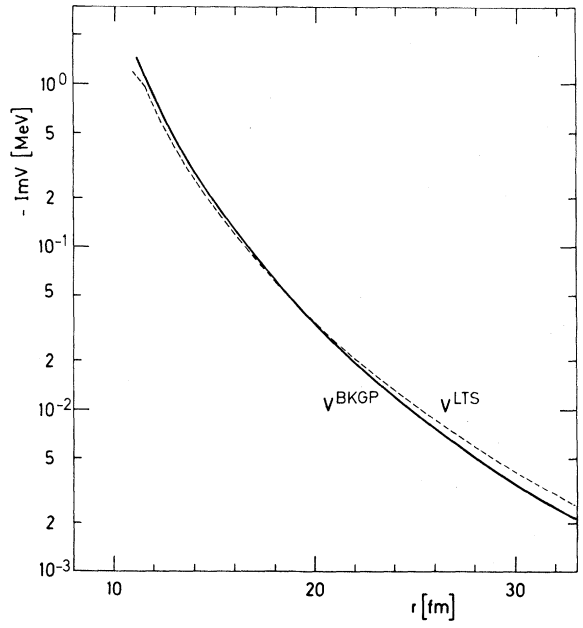

FIG. 2. The l-independent equivalent $V^{\mathrm{BKGP}}(r)$ of the l-dependent BKGP potential (Ref. 5) (solid curve) and the LTS potential (Ref. 4) $V^{\mathrm{LTS}}(r)$ (dashed curve) for $^{18}\mathrm{O}+^{184}\mathrm{W}$ at $E = 90$ MeV.

exists. It is in cases such as these where the inversion method is most helpful.

The de Boer–Winther scattering function S_l, calculated in a rotor model with $B(E2) = 1.3\times10^5$ MeV fm^2, is shown in Fig. 3(a). Its form is affected appreciably by excitations up to the 18^+ state. It is therefore clear that it deviates significantly from the corresponding LTS result.

The function $S = S(\lambda)$ is again fitted extremely well by expression (1), with $N = 7$. The resulting polarization potential $V(r)$ is shown in Fig. 3(b). The discrepancy between the imaginary part of $V(r)$ and the LTS potential is quite large outside the nuclear absorption region, $r \gtrsim 12$ fm. Figures 2(a) and 2(b) show that for the system under consideration, the higher-order couplings lead to a strong reduction of the absorption at shorter distances, as compared with the single-excitation mechanism. In contrast to the single-excitation case, ReV is here larger than ImV over a sizable range. (Inside the nucleus, the polarization potential V should be taken with caution, since the de Boer–Winther procedure disregards nuclear effects.)

The discrepancy between the single- and multiple-excitation potentials is also reflected in the corresponding elastic cross sections [Fig. 3(c)],

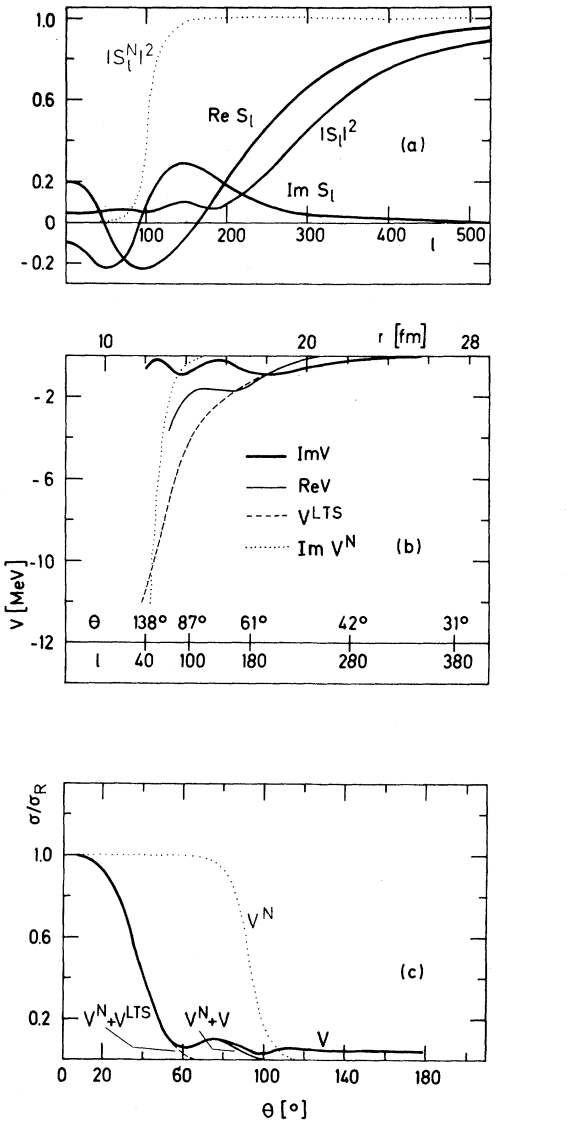

FIG. 3. The system $^{40}\mathrm{Ar}+^{238}\mathrm{U}$ at $E = 240$ MeV. (a) Scattering function: The solid curves show the real and imaginary parts of the elastic component S_l of the Coulomb-excitation S matrix as well as the corresponding reflection function $|S_l|^2$; the dotted curve represents the nuclear reflection function $|S_l^N|^2$ computed from a typical nuclear potential V^N with Woods-Saxon parameters $V = 43.20$ MeV, $W = 56$ MeV, $r_0 = 1.196$ fm, $a = 0.529$ fm. (b) Potential: The solid curves show the real and imaginary parts of the potential V computed by inversion of S_l; for comparison, the dashed curve shows the LTS potential V^{LTS}, and the dotted curve, the imaginary part of the nuclear potential V^N. (c) Cross section: The heavy solid curve shows the elastic cross section corresponding to V alone; the dotted curve represents the cross section computed from V^N alone, while the thin solid line shows the elastic cross section corresponding to $V+V^N$; for comparison, the dashed curve is computed from $V^{\mathrm{LTS}}+V^N$.

which differ for $\theta \gtrsim 50°$; the cutoff due to nuclear absorption occurs only at angles larger than $\sim 100°$. It would be interesting to have experimental data which show evidence of such multiple-excitation effects in the elastic cross section. Hopefully, appropriate scattering experiments with sufficient resolution can be carried out in the near future.

We remark that rather different sets of α_n, β_n fit a given scattering function with equal accuracy. However, the corresponding potentials calculated by inversion *all coincide.*

For the application of the polarization potential in the calculation of scattering and absorption cross sections, or of the absorption along given trajectories, it would evidently be useful to devise a simple parametrization of the potential whose parameters would have to be determined by systematic studies. For the absorptive part, one might consider on LTS-type behavior with a leveling off at small distances.

The authors thank B. Bohne for programming and carrying out the numerical calculations.

[1]D. J. Weber, M. A. Franey, D. Dehnhard, J. L. Artz, V. Shkolnik, and N. M. Hintz, Bull. Am. Phys. Soc. 21, 1006 (1976).

[2]C. E. Thorn, M. J. LeVine, J. J. Kolata, C. Flaum, P. D. Bond, and J. -C. Sens, Phys. Rev. Lett. 38, 384 (1977).

[3]P. Doll, M. Bini, D. L. Hendrie, S. K. Kauffmann, J. Mahoney, A. Menchaca-Rocha, D. K. Scott, T. J. M. Symons, K. van Bibber, Y. P. Viyogi, H. Wieman, and A. J. Baltz, Phys. Lett. 76B, 556 (1978).

[4]W. G. Love, T. Terasawa, and G. R. Satchler, Nucl. Phys. A291, 183 (1977), and Phys. Rev. Lett. 39, 6 (1977).

[5]A. J. Baltz, S. K. Kauffmann, N. K. Glendenning, and K. Pruess, Phys. Rev. Lett. 40, 20 (1978).

[6]Cf., e.g., G. Baur, F. Rösel, and D. Trautmann, Phys. Rev. C 17, 2256 (1978).

[7]Cf., e.g., J. de Boer and Aa. Winther, in *Coulomb Excitation*, edited by K. Alder and Aa. Winther (Academic, New York, 1966).

[8]R. Lipperheide and H. Fiedeldey, Z. Phys. A 286, 45 (1978).

[9]W. H. Miller, J. Chem. Phys. 51, 3631 (1969).

[10]E. Kujawski, Phys. Rev. C 6, 709 (1972), and 8, 100 (1973).

Coriolis-Distorted Bands of Common $g_{9/2}$ Parentage in Odd and Doubly Odd $N = 41$ Nuclei

A. J. Kreiner and M. A. J. Mariscotti

Departamento de Física, Comisión Nacional de Energía Atómica, Buenos Aires 1429, Argentina

(Received 26 June 1979)

All features of a $\Delta I = 1$ band displaying Coriolis-like distortions based on a 4^+ isomeric state, recently discovered in ^{76}Br, are successfully described within the framework of a two-noninteracting-quasiparticle–plus–rotor calculation. Assuming the intrinsic state to be of $\tilde{\pi}g_{9/2} \otimes \tilde{\nu}g_{9/2}$ parentage it is possible to account in a natural way for the apparent relationship noted between this 4^+ state and the $\frac{5}{2}^+$ ground-state band of the neighboring isotone ^{77}Kr.

In recent years, the study[1-7] of high-spin states in transitional doubly odd nuclei has revealed the occurrence of certain interesting phenomena. One of these concerns Coriolis-distorted band structures found in the $N = 41$ doubly odd nuclei ^{76}Br (Ref. 2) and ^{78}Rb (Ref. 4) and their apparent relationship with the $\frac{5}{2}^+$ ground-state band[8] in the intermediate isotone ^{77}Kr. The first two excited states in these bands lie nearly at the same energy as the corresponding levels in the ^{77}Kr band, and while the higher levels in the doubly odd nuclei become depressed relative to those in ^{77}Kr, the phase of the level staggering remains the same. This observation[2,4,9] seems to imply that the coupling of a certain proton excitation to the ^{77}Kr ground-state band does not alter significantly the structure of this band's low-lying spectrum.

The theoretical investigation of this problem met with success only after the recent discovery[9,10] of a 4^+ isomer in ^{76}Br and the assignment of this state as the band head[9] (instead of the 1^- ground state as hitherto thought[2]). Earlier attempts in this direction showed that it was not possible to reproduce such a band if it was built on a low-spin, negative-parity state, a result which partially motivated the search[9] for an isomer in ^{76}Br.

In this Letter we wish to present an interpretation of these band structures, based on the two-noninteracting-quasiparticle–plus–rotor model,[6]

